# PFAS destruction and near complete defluorination of undiluted aqueous film-forming foams at ambient conditions by piezoelectric ball milling

Nanyang Yang,[1] Yunqiao Guan[1], Shasha Yang,[1,2] Caitlyn Olive,[1] Sujan Fernando,[1] Thomas M. Holsen,[1] Yang Yang[1]*

[1] Department of Civil and Environmental Engineering, Clarkson University, Potsdam, New York 13699, United States

[2] Institute for a Sustainable Environment, Clarkson University, Potsdam, New York 13699, United States

* Corresponding author: Email: yanyang@clarkson.edu; Tel: +1-315-268-3861

## ABSTRACT

The non-thermal destruction of aqueous film-forming foam (AFFF) stockpiles, one of the major culprits responsible for water and soil contamination by per- and polyfluoroalkyl substances (PFAS), is extremely challenging because of the coexistence of mixed recalcitrant PFAS and complicated organic matrices at extremely high concentrations. To date, the complete defluorination of undiluted AFFF at ambient conditions has not been demonstrated. This study reports a novel piezoelectric ball milling (BM) approach for treating AFFF with a total organic fluorine concentration of 9,080 mg/L and total organic carbon of 234 g/L. Near-complete defluorination (> 95% conversion of organofluorine to fluoride) of undiluted AFFF was achieved by co-milling with boron nitride (BN). By carefully examining the experimental data, we identified AFFF liquid film thickness (Z) at the collision interface as a descriptor of treatment performance. We further validated that effective defluorination proceeded when Z was less than a criteria value of 2.3 μm. In light of this new understanding, the addition of $SiO_2$ as a dispersant and the pre-evaporation solvents to reduce Z have been validated as effective strategies to promote AFFF treatment capacity.

## Introduction

Per- and polyfluoroalkyl substances (PFAS) are synthetic chemicals used since the 1940s.[1] Their ubiquitous presence in the environment, significant toxicity, and persistence have raised growing public concerns.[2] Aqueous film-foaming foam (AFFF) was identified as the major culprit responsible for the elevated PFAS concentration in the receiving water and soil of manufacturing sites, airports, and military fire training areas.[3–5]

The most urgently needed proactive solution to curb new PFAS contamination from using AFFF is the disposal of the existing chemical stockpile. The incineration of AFFF is facing regulatory challenges due to concerns about the emission of incomplete combustion products and greenhouse gas.[6,7] Alternative non-thermal technologies enabling near-complete defluorination (i.e., conversion of organofluorine on PFAS to fluoride ($F^-$)), in addition to degradation of parent PFAS compounds, are desired to meet the zero PFAS pollution goal.[8] However, deep defluorination of even a single type of PFAS is challenging. For instance, the maximum defluorination efficiencies of treating perfluorooctane sulfonic acid (PFOS) by electrochemical oxidation, UV-sulfite photoreduction, and alkaline-assisted heat treatment are below 80%.[9–11] The deep defluorination of AFFF, a mixture of concentrated PFAS with co-existing solvents and surfactants, [12,13] is a next-level challenge that has been inadequately addressed.

The past investigations of PFAS defluorination were heavily invested in the treatment of model PFAS, with only a few studies that used electrochemical oxidation, plasma, advanced oxidation, and UV-sulfite photoreduction to treat diluted AFFF with total fluorine (**TF**) ranging between 0.1-27 mg F/L.[13–17] All these technologies demonstrated structurally dependent reactivity in removing target PFAS, and none achieved near-complete defluorination. To date, only hydrothermal alkaline treatment realized ~100% defluorination of AFFF but demands high temperature (170-350°C), pressurized reactors (2-22 MPa), and alkaline addition (5 M of NaOH).[18]

Ball milling (**BM**) is an emerging technology for destroying PFAS chemicals at ambient conditions. Using potassium hydroxide (KOH) as a co-milling reagent destroys perfluorooctanoic acid (**PFOA**) and perfluorooctane sulfonic acid (**PFOS**).[19,20] However, the residual KOH in the media must be neutralized before discharge. Using quartz sand ($SiO_2$) as a neutral reagent to destroy PFAS is possible. However, the degradation kinetics are slower, and the fluoride yield is low.[20,21] Previously, we discovered that boron nitride (**BN**), a piezoelectric material, can be activated in the BM process to generate ~kV potential to destroy solid PFAS.[22] Building upon this

early success, this study reports unprecedented results that the BN-assisted BM (**BN-BM**) can achieve ~100% defluorination of undiluted liquid AFFF with a TF concentration of 9,080 ± 180 mg/L (vs. 0.1-27 mg/L reported previously[13–17]). We further developed a critical liquid film theory to guide the process scale-up. The critical insights of this study established a novel AFFF treatment paradigm and expanded the applications of piezoelectric BM from solid chemical destruction to liquid waste disposal.

**Comprehensive analytical approaches to close the fluorine balance.**

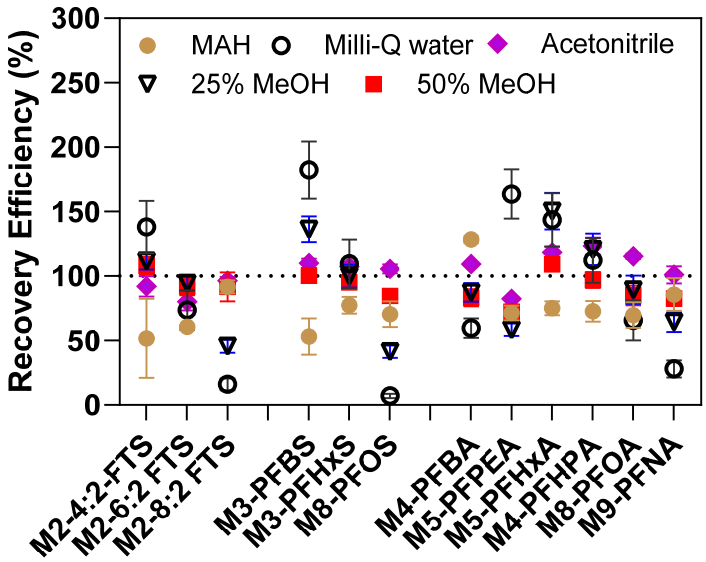


**Figure 1.** Comparison of the extraction recovery efficiencies of isotope-labelled PFAS using various solvents. The prefix "M#" refers to the number of carbons labeled by $^{13}C$. An isotope-labeled PFAS mixture (40 µL of 1000 ng/mL for individual PFAS) was spiked in 100 mg BN. Data are presented as means of triplicates ± standard deviation.

This study developed a novel BN-BM process for the treatment of liquid AFFF. The AFFF was found to contain 11 PFAS with different function groups and chain lengths and other unknown fluorocarbons (Table S1; to be discussed in the following content). Therefore, it was critical to identify a solvent that would ensure the effective extraction of all target PFAS from the milled samples (slurry-like samples for AFFF treatment). To determine this, we spiked twelve isotope-labeled PFAS (fluorocarbon number, n=3-9; each PFAS has a concentration of 1000 µg/mL) into

the BN powder. The mixture was ultrasonically extracted using various solvents, including 0.3% methanolic ammonium hydroxide (MAH; a solvent recommended by EPA Draft Method 1633[25]), Milli-Q water, 25% methanol (MeOH), 50% MeOH, and acetonitrile with 0.2% formic acid (details are provided in Text S1). MeOH (50%) was the best-performing solvent, with recoveries of PFAS with various structures from 80-110% (Figure 1).

Demonstrating the near-complete defluorination of individual PFAS and AFFF is the only evidence that can be used to confirm PFAS mineralization and mitigated risk. In this study, the PFAS destruction efficiency and degree of defluorination were based on the decay in PFAS concentrations and the quantitative yield of $F^-$ measured in extract solvents using both $F^-$ and total organic fluorine (TOF). The defluorination efficiency (**DeF**) was calculated as:

$$\text{DeF}\ (\%) = ([F^-]_t - [F^-]_0)/([\text{TOF}]_0\text{-}[\text{TOF}]_t) \times 100\% \quad (1)$$

where $[F^-]_0$ and $[F^-]_t$ are the molar mass of $F^-$ in the extract solutions of samples before and after BM treatment, respectively. $[\text{TOF}]_0$ and $[\text{TOF}]_t$ are the molar mass of TOF before and after BM treatment, respectively. For the destruction of analytical-grade PFAS chemicals, TOF is the product of fluorine number and the parent PFAS concentration. The $[\text{TOF}]_0$ of AFFF was given by the combination of CIC and IC analyses as described in the methods section. With the detection limits of $[F^-]$ by IC of 50 μg/L, $[\text{TOF}]_t$ down to the levels of nmol/L (based on targeted PFAS analysis) and μmol/L (based on CIC measurements), the highly sensitive and comprehensive analytical approaches were sufficient to determine if near-complete defluorination, arbitrarily defined as DeF > 95% was achieved.

**Near-complete defluorination of individual PFAS.**

Using BN as a typical piezoelectric material, we demonstrated that piezoelectric BM achieved complete defluorination of PFOS and PFOA.[22] Further, we demonstrated that the BN-BM process outperformed BM using KOH, as evidenced by the faster PFAS destruction kinetics and higher DeF. Quartz sand ($SiO_2$) has also been demonstrated to have reactivity in removing PFAS, although < 20% defluorination efficiency was observed for PFOS and PFOA.[19,20] Gobindlal et al. used solid-state nuclear magnetic resonance (**NMR**) spectroscopy to show that insoluble Si-F bonds were formed by this process, which explained the low recovery of $F^-$ by solvent extraction in these experiments.[21] However, as a semi-quantitative approach, NMR analysis cannot exclude

the possibility that unextractable or unknown fluorocarbon residues were also formed but were below the instrument detection limit or not detected using traditional analyses.

In this study, PFAS chemicals or undiluted AFFF (discussed later) were added to 100 mL stainless steel jars filled with SS balls (16 Ø1.0 cm large balls and 100 Ø0.6 cm small balls; 160 g in total) and co-milling reagents (0.4-6.0 g; details disclosed below). The planetary disk and jars were rotated at 290 and 580 rpm, respectively. All BM treatment tests were conducted at room temperature and atmospheric pressure.

Figures 2a-c compare the performance of BN− and $SiO_2$−BM processes on the destruction and defluorination of 6:2 fluorotelomer sulfonate (FTS), PFOA, and PFOS. The BN-BM treatment used a [BN] vs. [F on PFAS] molar ratio of 5:1, as optimized previously[22], while the $SiO_2$−BM treatment adopted a [$SiO_2$] vs. [F on PFAS] molar ratio of 20:1. Even though the molar dosage of BN was one-fourth that of $SiO_2$, BN still exhibited significantly faster removal kinetics for all PFAS than $SiO_2$ alone. BM treatment using a combination of BN and $SiO_2$ ([BN+$SiO_2$]−BM) showed that the addition of $SiO_2$ did not promote PFAS destruction, suggesting that BN-mediated destruction is the dominant mechanism in [BN+$SiO_2$]−BM treatment.

Previously, we reported the formation of short-chain perfluoroalkyl carboxylic acids (PFCAs) intermediates in the BN−BM treatment of PFOA and PFOS.[22] This study provides new information for 6:2 FTS destruction. The BN−BM treatment of 6:2 FTS yielded C4-6 PFCAs (Figure S1a). The formation of dominant intermediate perfluorohexanoic acid (PFHxA) indicates the cleavage of C−C bonds of the $-CF_2-CH_2-$ moieties. The further destruction followed the $-CF_2-$ stepwise elimination pathway to form shorter-chain PFCAs until mineralization. The intermediate profiles suggest the reaction followed a series of direct electron transfer oxidation of PFAS by the transient high piezoelectric potentials on BN activated by BM.[22] Other aspects of the reaction have already been revealed in our previous study:[22] (1) BN was converted to $NH_4^+$ and $BO_3^-$; (2) $F^-$ derived from destroyed PFAS was bound by $NH_4^+$ to form soluble $NH_4F$; (3) oxygen in air-sealed in the jar is likely to be the electron acceptor in the oxidative destruction of PFAS.

The $SiO_2$−BM process may follow a different reaction pathway: BM results in the homolytic cleavage of Si−O bonds in quartz to form silyl (≡Si•) and siloxyl (≡Si−O•) radicals,[26] which generate •OH (≡Si−O• + $H_2O$→≡Si−OH + •OH) and •H ((≡Si• + $H_2O$→ Si−OH + •H) via hydrolysis by moisture.[21,27] Due to the recalcitrance of most PFAS to •OH attack, reductive H/F exchange defluorination facilitated by •H is believed to be the dominant destruction pathway.[26,28]

As proven in photochemical reductive defluorination studies,[10,29] the H/F exchange followed by hydrolysis or radical attack can also produce PFCAs, which explains the formation of PFCA intermediates in the $SiO_2$–BM process (Figure S1b). Further investigation of this process was beyond the scope of this study.

[BN+$SiO_2$]–BM treatment of 6:2 FTS, PFOA, and PFOS yielded PFCAs intermediates with peak concentrations higher than $SiO_2$-BM but lower than BN–BM (Figure S1c and S2). In general, BM reactions involving $SiO_2$ exhibited lower DeF (discussed below).

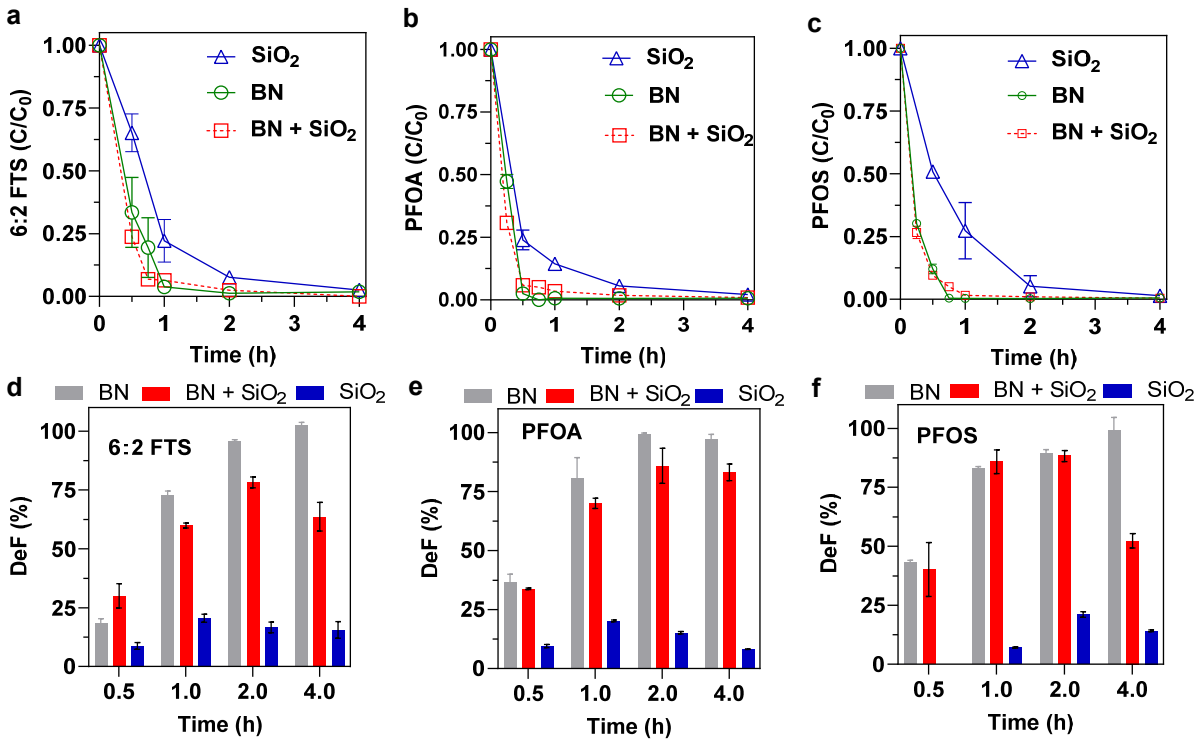


**Figure 2**. Decay of (**a-c**) parent PFAS and (**d-f**) defluorination with different co-milling reagents during BM treatment. The initial mass of 6:2 FTS, PFOA, and PFOS were 0.3, 0.23, and 0.23 mmol, respectively. For all tests using BN and $SiO_2$ separately or combined, the molar ratio of [BN] vs. [F on PFAS] was 5:1; the molar ratio of [$SiO_2$] vs. [F on PFAS] was 20:1. Data are presented as mean values of triplicates ± standard deviation.

The BN–BM treatment readily achieved > 98% DeF for 6:2 FTS, PFOA, and PFOS (Figures 2d-f; raw data see Table S2), while less than 25% DeF was observed in experiments using only $SiO_2$. For the [BN+$SiO_2$]–BM process, the DeF values were much larger than when using $SiO_2$

alone but lower than BN−BM. Moreover, DeF appeared to decrease after reaching peak values, likely because extended milling resulted in $F^-$ reacting with $SiO_2$ to form unextractable Si−F species. Overall, these results suggest that BN is largely responsible for the PFAS breakdown to $F^-$. It seems $SiO_2$ does not promote the BN-BM treatment of solid PFAS chemicals. However, as will be revealed below, the promotional role of $SiO_2$ became significant in liquid AFFF treatment.

**Near-complete defluorination of undiluted AFFF.**

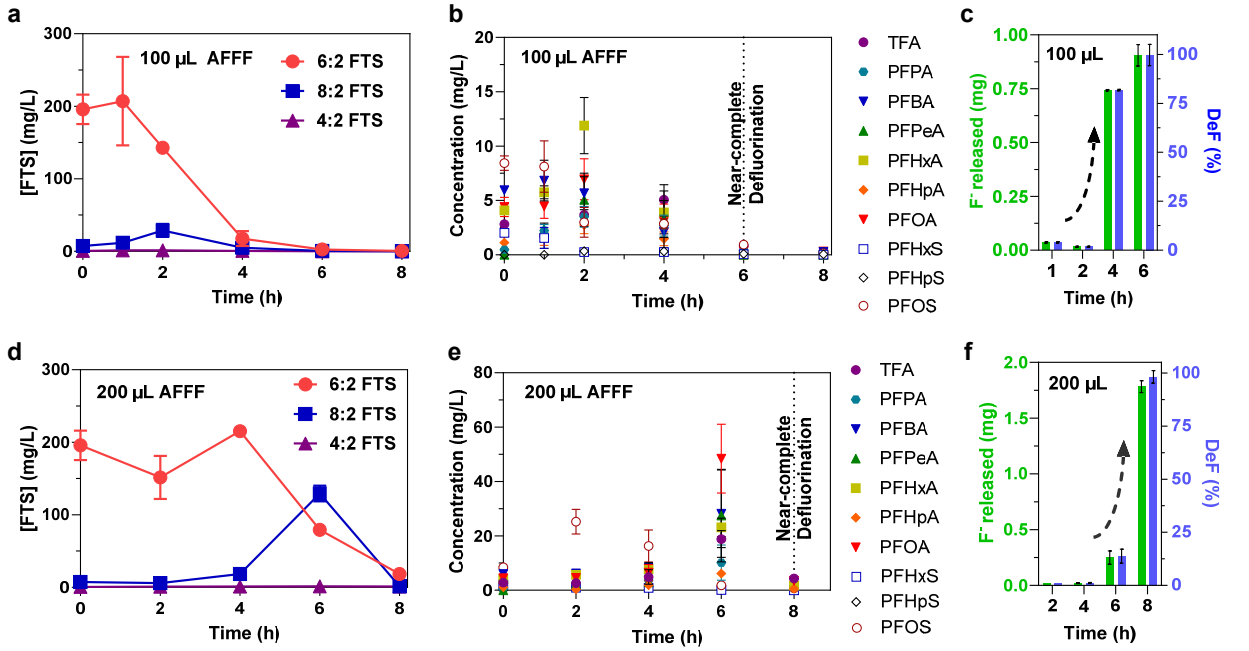


**Figure 3.** Time profiles of (**a**) FTS, (**b**) other PFAS, and (**c**) defluorination in the BM treatment of 100 µL AFFF with 0.5 g BN as the co-milling reagent. Time profiles of (**d**) FTS, (**e**) other PFAS, and (**f**) defluorination in the BM treatment of 200 µL AFFF with 0.5 g BN as the co-milling reagent. The ball mill jar rotation speed was 580 rpm. Data are presented as mean values of triplicates ± standard deviation.

To date, only a few studies have reported on the destructive treatment (EO, UV/S, and plasma) of diluted AFFF at ambient conditions.[14–17,30] In those studies, the total fluorine concentrations were mostly estimated either using the total oxidizable precursor array (TOPA) analysis or NMR as 0.16-27 mg/L, and the DeF ranged from 50-81% (Table S3).

AFFF could be manufactured by electrochemical fluorination (ECF) or fluorotelomerization (FT) methods. The manufacture of ECF-derived AFFF has been discontinued since 2002.[31] Therefore, this study focused on the treatment of FT-derived AFFF, which is responsible for telomer-dominant PFAS contamination in water and soil.[5,32,33] The targeted analysis of 30 PFAS in the AFFF identified 6:2 FTS (175.5 mg/L) as the dominant PFAS, along with 8:2 FTS, PFCAs, and perfluorosulfonic acid (PFSAs). The TOF was 9,080 mg/L (Table S2). The fluorine on target PFAS (121.7 mg/L) only makes up 1.3% of the TOF, suggesting the existence of massive amounts of unidentified fluorocarbon components. The rich organic matrix contributed to an extremely high total organic carbon (TOC) of 234 g/L.

AFFF was treated as received without dilution. Milling 0.5 g BN with 100 μL of AFFF (TOF=47.8 μmol) led to the destruction of FTS, accompanied by the generation and decay of PFCAs (Figures 3a and b). A series of $n$=6−7 PFAS surfactant precursors were detected by Q-ToF-HRMS following the literature (Figure S3).[18] The destruction of 6:2 FTS, 8:2 FTS, and precursors via the cleavage of $-CF_2-CH_2-$ or $-CF_2-SO_2-$ followed by the hydrolysis of the terminal $-CF_2\bullet$ to −COOH may explain the formation of PFHxA and PFOA as intermediates. Targted PFAS and precursors were destroyed after 6 h of reaction (Figure 3a, 3b, and S3). Achieving bulk defluorination (*i.e.*, all TOF broken down to $F^-$) of AFFF is more challenging than destroying target PFAS due to the complexity of the AFFF solution. Surprisingly, after 6 h of BM treatment, >99% defluorination of AFFF was achieved (Figure 3c; see Table S2 for fluorine balance data). This is the very first proof-of-concept demonstrating the near complete defluorination of AFFF via a novel piezoelectric BM route.

We further investigated the performance of the BN−BM process in treating a doubled amount of AFFF (200 μL; TOF=95.6 μmol). Significant PFAS destruction was observed after 6 h (Figures 3d and e). More than 98% defluorination was still achieved after a prolonged treatment duration of 8 h (Figure 3f and Table S2). These results imply that the BM process has a high robustness toward AFFF loads. More importantly, it was noted that an "incubation period" was required before significant defluorination (arbitrarily defined as DeF>50%). Specifically, the destruction of PFAS and $F^-$ yield abruptly accelerated after 4 and 6 h for the treatment of 100 and 200 μL AFFF, respectively. This positive correlation between AFFF loads and the incubation period was not observed in the BM treatment of individual solid PFAS (Figure 2), revealing mechanistic insights into the process as discussed below.

## Critical liquid film thickness.

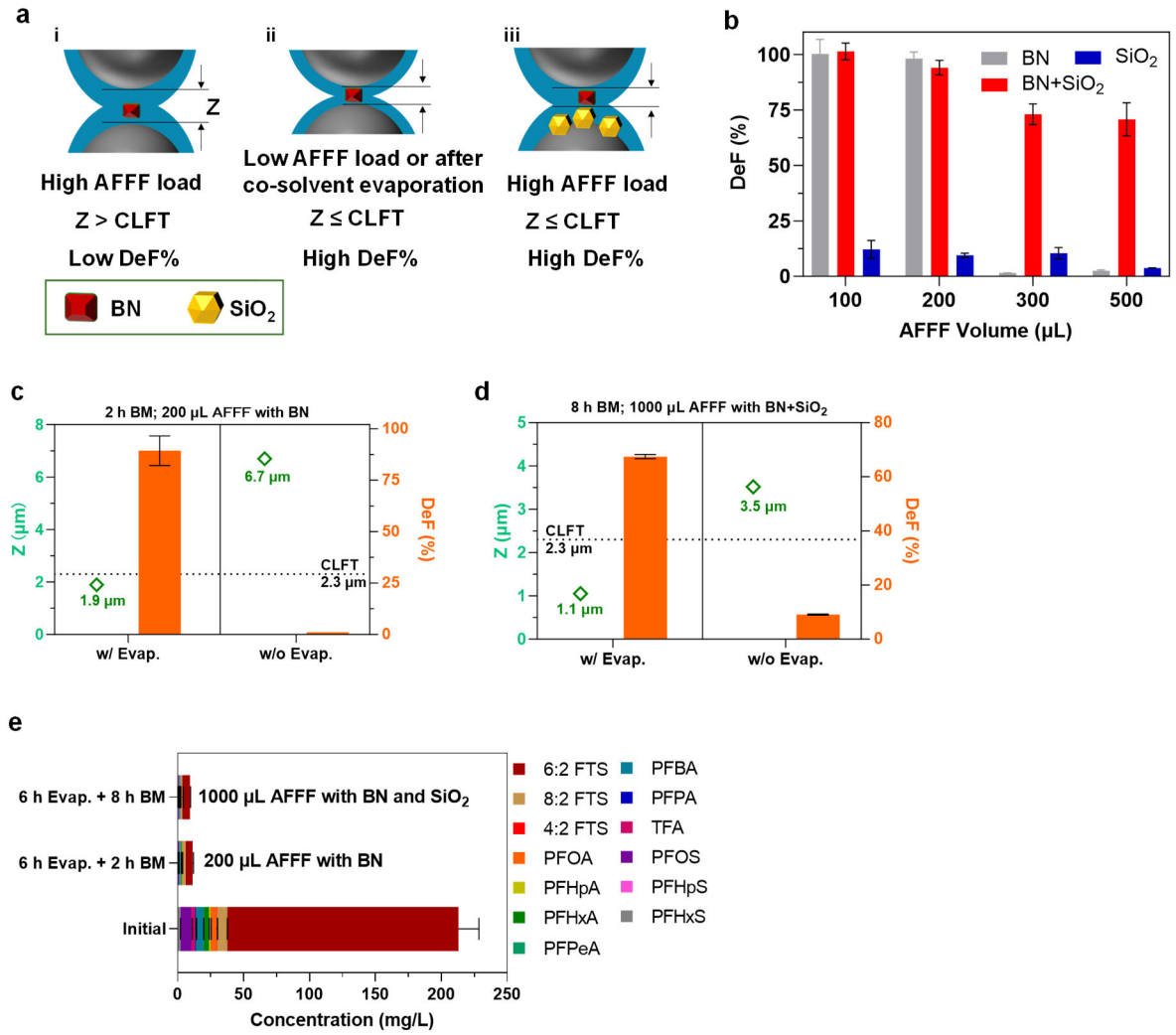


**Figure 4.** (**a**) Schematic illustrations of the CLFT theory. (**b**) Defluorination efficiency (DeF) after 8 h BM treatment of various volumes of AFFF. (**c**) Comparison of DeF and Z values of treating 200 μL AFFF with or without evaporation (Evap) pretreatment using 0.5 g BN as a co-milling reagent. (**d**) Comparison of DeF and Z values of treating 1000 μL AFFF with or without Evap pretreatment using 0.5 g BN and 5 g $SiO_2$ as co-milling reagents. (**e**) PFAS destruction with Evap pretreatment. Evap pretreatment was performed by placing the AFFF-loaded ball mill jar in a water bath at 60 °C for 6 h with the lid open.

As discussed in our previous study, the BM process is driven by the impact force provided by ball collisions.[22] In general, BM of wet media yields a lower impact force than dry BM due to the presence of liquid phases that incur drag forces in the counter direction of impact.[34] We hypothesize that due to its surfactant-like nature, AFFF should be uniformly coated on the surfaces of balls and jar walls at a certain liquid film thickness (**Z**). Further, we propose that there is a critical liquid film thickness (**CLFT**) so that when Z > CLFT (Figure 4a-i), the drag force offsets the impact force enough to retard PFAS destruction. The delivery of impact energy to BN and the consequent PFAS destruction is only effective when Z < CLFT (Figure 4a-ii).

The mechanochemical process may generate transient high temperatures at the point of collision or friction.[35] However, the possibility of PFAS pyrolysis in our system was excluded as the milling of PFAS in the absence of BN did not lead to destruction.[22] The ball surface temperature measured immediately after different durations of BM using an infrared thermometer was 60 ± 4 °C. This value is far below the minimum criteria (> 200 °C) of thermal decomposition of PFAS,[36] but it might be sufficient to vaporize co-solvents in AFFF. Since it is impossible to study the solvent vaporization process when AFFF was blended with co-milling reagents in a fast-moving jar, we placed AFFF samples in a water bath held at a constant 60°C to simulate heat-induced solvent loss. The heating led to volume reduction linearly correlated with heating time (Figure S4a). The 4 h heating resulted in a 38% volume reduction, and the sum of target PFAS concentrations in the remaining AFFF solution increased by 37% correspondingly (Figure S4b**).** These results indicate that heating only led to a loss of co-solvent with PFAS remaining in the liquid phase.

Driven by the liquid film hypothesis discussed above, we took a closer look at the BN−BM treatment of 100 µL of AFFF. Assuming a uniform coating of AFFF on the stainless steel balls (164 $cm^2$) and jar walls (104 $cm^2$), 100 µL of AFFF in the mill should have an initial Z ($Z_0$) of 3.7 µm. Taking the data of heat-induced solvent loss measurement into consideration, a 4 h BM treatment (equivalent to being heated at 60 °C for 4 h) should lead to a 38% volume reduction and reduce Z to 2.3 µm. Because the steep rise in DeF was also observed at 4 h milling (Figure 3c), we conclude that Z of 2.3 µm is the CLFT. The CLFT of 2.3 µm is commensurate with the sizes of the BN particles at 1-2 µm (Figure S5). This observation suggests that significant defluorination occurs when BN particles receive direct ball impact with minimum shielding of the liquid film (Figure 4a-ii).

The CLFT theory can be used to explain the extended defluorination incubation period in treating 200 µL AFFF. The $Z_0$ of 200 µL AFFF was calculated to be 7.5 µm. According to the ex-situ heating tests (Figure S4), the volume reduction at 4, 6, and 8 h is projected to be 38, 56, and 75%, corresponding to Z values of 4.6, 3.3, and 1.9 µm, respectively. Only Z of 1.9 µm is less than CLFT, which explains the sharp increase of DeF at 8 h (Figure 3f).

It is important to point out the caveats of the CLFT theory.

(1) We intentionally excluded the surface area of BN (37 $m^2/g$ measured by $N_2$-BET) in the Z value calculation. This is because BN has hydrophobic surfaces.[37,38] It cannot be completely wetted by AFFF (Figure S6a). Therefore, BET surface area accessible to $N_2$ molecules does not represent the actual effective area interacting with AFFF (which is impossible to measure experimentally). This assumption also means that the Z value is a descriptor of the collision environment provided by the ball milling system (jars, balls, and inert dispersants) independent of reagent properties. Consequently, the model can be universally applicable to other piezoelectric co-milling reagents.

(2) Approximately 50% of the TOC of AFFF remained after BN−BM treatment (Figure S7), indicating that the BN-BM process destroys a portion of the co-solvent, and the undestroyed vaporized co-solvent was contained in the sealed jar and recondensed after the treatment. If this was not the case, a more significant loss of TOC should be expected. Given a ~100% DeF was achieved, the release of gaseous PFAS or other F-containing compounds should not be significant. However, this needs to be verified in future experiments.

(3) The ex-situ measurement of heat-induced volume reduction (Figure S4) was performed in an open system for ease of tracing weight changes and calculating the volume reduction (assuming the density remained constant). In contrast, in the BM treatment, the jar was sealed, where co-solvent evaporation may be inhibited by higher partial pressures than in an open system, corresponding to a slower reduction of liquid film thickness. Therefore, the value of CFLT needed for BM treatment may be slightly larger than that estimated above. Nonetheless, the CFLT theory is sufficient to guide the process improvement.

**Promote treatment capacity based on the CLFT theory.**

The BN−BM process provides a novel solution to realize the near-complete defluorination of AFFF at ambient conditions. Guided by the CLFT theory, we further developed two strategies to promote the AFFF treatment capacity.

The first approach is to increase the surface area for collision. We used $SiO_2$ as the addictive solid media to augment the collision surface as it provides a hard surface (Mohs scale hardness of 7 for $SiO_2$ and 8 for stainless steel),[39,40] but at a much lower cost.

The control test using $SiO_2$ as the only co-milling reagent to treat 200 μL AFFF shows that the target PFAS concentrations increased after BM treatment (Figure S8a). This result implies that the $SiO_2$−BM can only break down precursors to target PFAS, while further mineralization was non-existent or very slow. Consequently, the defluorination was insignificant (DeF < 10%; Figure S8b). On the other hand, using BN could realize deep defluorination of AFFF, but the process failed to treat AFFF at a volume higher than 200 μL (Figure 4b). Surprisingly, the BM using the combination of BN and $SiO_2$ (e.g., [BN+$SiO_2$]–BM) achieved > 70% defluorination when treating up to 500 μL AFFF (Figure 4b).

The synergy of BN and $SiO_2$ can be explained by the CLFT theory. As shown in Figure S6b, AFFF can be dispersed on $SiO_2$ particles because of their hydrophilic surfaces. The $SiO_2$ (Ø 250 μm) mainly served as dispersants to provide an extra 453 $cm^2$ collision area (Text S2). When amended with 5 g $SiO_2$, the $Z_0$ for treating 100 and 200 μL of AFFF are 1.4 and 2.8 μm, smaller than or close to the CLFT. Therefore, efficient PFAS destruction and defluorination were facilitated since the beginning of [BN+$SiO_2$]–BM treatment, which explains the elimination of the incubation period compared with the BN-BM process (Figure S9 vs. Figure 3f). As for treating 300 and 500 μL AFFF with $Z_0$ of 4.2 and 6.9 μm, the Z's were reduced to 1.0 and 1.7 μm, respectively, after 8 h of reaction. Thus, the high DeF observed at this treatment time can also be attributed to Z < CLFT.

The second strategy to promote treatment capacity is to reduce $Z_0$ by pre-evaporating the solvents in AFFF before BM treatment. As shown in Figure 3f, the BN-BM treatment of 200 μL AFFF for 2 h led to a negligible DeF. We found that preheating the jar (lid opened) at 60 °C for 6 h followed by a 2 h BN−BM treatment achieved > 90% DeF (Figure 4c) and > 94% of target PFAS destruction (Figure 4e). The results of these two treatment scenarios with and without pre-evaporation can be explained by the CLFT theory: The heat effects of 2 h BM treatment can only reduce the Z value from 7.5 to 6.7 μm, which is still larger than CLFT. Thus, the PFAS destruction did not proceed effectively. However, including 6 h pre-evaporation (solvents released to air) followed by 2 h BM treatment (solvents vaporized in the jar) provided an 8 h heat-induced solvent

loss. These approaches reduced the Z to 1.9 μm (< CLFT of 2.3 μm). Thus, a high DeF can be expected for the latter scenario.

Last, we showcase an example of combining two strategies (i.e., introducing evaporation pretreatment and increasing collision surface) to treat 1000 μL AFFF. AFFF (1000 μL) spiked in the BN+$SiO_2$ system should have a $Z_0$ of 13.9 μm. The BM treatment without pre-evaporation should reduce the Z value to 3.5 μm (> CLFT) after 8 h. Therefore, low DeF was observed at this point. In contrast, a tandem process including 6 h pre-evaporation followed by 8 h BM treatment incurred 14 h of heat-induced solvent loss. The Z was estimated to be 1.1 μm (< CLFT), which explains the significant DeF of > 60% (Figure 4d). It is of note that > 90% destruction of target PFAS was achieved (Figure 4e). However, $SiO_2$ may immobilize part of the $F^-$, prohibiting the treatment from demonstrating a higher DeF.

**Environmental Applications.**

This is the first study to demonstrate the deep defluorination of liquid undiluted AFFF by piezoelectric BM at ambient temperatures and pressures. The innovation addressed the critical need for non-thermal AFFF treatment. Our fundamental contribution is to identify CLFT as the critical descriptor for the BM treatment of liquid waste. We present a closed-loop research workflow of building the CLFT theory based on experimental data and, in return, using the theory to guide the process improvement.

The addition of inert dispersant (e.g., $SiO_2$) to provide extra collision surfaces and the pre-evaporation of solvents were demonstrated as two feasible options to promote AFFF treatment capacity. Evaporation could be realized on commercial evaporators using waste heat or solar energy. It is important to note that evaporation was introduced as an example. Other PFAS concentration approaches could also be adopted. As for the BM treatment, we used 100 mL jars filled with BN (0.5 g) and $SiO_2$ (5 g) at a balls/reagents mass ratio of 29 to treat 100-1000 μL AFFF. We previously calculated that the force induced by steel ball collision in our planetary ball mill is 57 N.[22] These parameters lay the groundwork for the optimization and design of scaled-up systems in our following studies. Should these parameters (impact force, balls to feedstock mass ratio, [BN mass]/[AFFF volume] ratio, etc.) be reproduced on a commercial ball mill and the CLFT criteria be met, the on-site disposal of large volume undiluted AFFF can be expected.

The BN−BM process shows high durability as it can destroy PFAS in the presence of extremely high ~200 g/L TOC. The BN is a common commercial product. After the BM reaction, along with the mineralization of organofluorine to $F^-$, the reacted BN will be converted to ammonium and borate.[22] Even if released in the environment, BN is considered bio-compatible with non-cytotoxicity.[41] These unparalleled advantages empower the BN−BM process with the versatility to be integrated with various water treatment trains. Given its high tolerance to organic matrices, it may be able to destroy PFAS or other chemical contaminants in very concentrated waste (concentrated AFFF, desalination brine, dewatered bio-solid). Given that the process is driven by solid-solid phase collision, the BN–BM process is also promising for the destruction of PFAS on water treatment-derived sorbents (activated carbon, ion-exchange resins, etc.). Thses applications will be reported in our forthcoming studies.

## Methods

### Chemicals and ball milling reaction.

Detailed information on the chemicals used is provided in Text S3. AFFF (3% AFFF Buckeye MIL-SPEC) was treated as received. The BM treatment was conducted on a planetary ball mill (PQ-N04, Across International).

### Solvent extraction and PFAS analysis

In the tests of BM destruction of pure PFAS chemicals, the milled samples were ultrasonically extracted with 50 mL of solvent (Milli-Q water for PFOA and 6:2 fluorotelomer sulfonate; methanol for PFOS) for 15 min. In the treatment of AFFF, the milled sample containing co-milling reagent and AFFF was extracted using 50 mL of 50% MeOH. The mixture of solvents and solids was subjected to 15-min sonication and 6-min centrifugal separation at 5000 rpm. The resulting supernatant (*i.e.*, extract) was then diluted to 75% methanol by 10-100 times for instrumental analysis.

PFAS in extracts were analyzed using ultra-high-performance liquid chromatography (UPLC, Thermo Vanquish) coupled to a triple quadrupole mass spectrometer (MS/MS, Thermo Altis) in the Center for Air and Aquatic Reseach Engineering and Science at Clarkson University, a DoD accredited lab for PFAS analysis. A 10 μL sample was injected and then separated on a Thermo Scientific Hypersil GOLD PFP column (2.1 mm × 100 mm, 1.9 μm). Sample acquisition and

analysis were performed with TraceFinder 5.1 (Thermo Scientific). The setup of LC-MS/MS can be found in Text S4. Method detection limits of 30 PFAS were at ng/L levels, as tabulated in Table S1. Nontargeted analysis of PFAS precursors was conducted through a high-performance liquid chromatography-quadrupole time-of-flight mass spectrometry (HPLC/QToF-MS, SCIEX) in both ESI positive and negative modes. Details of the nontargeted analysis can be found in Text S5.

**Analysis of $F^-$, TOC, and TF.**

The BM-treated samples were extracted using Milli-Q water for the analyses of $F^-$ and TOC. $F^-$ in the extracts was analyzed by a Dionex Aquion chromatography system with an anion-exchange column (Thermo Fisher Scientific, RFIC™ IonPac™ AS18 column). The detection limit of $F^-$ was 50 μg/L. Quantification of TOC was conducted on a SHIMADZU TOC-L instrument that had a detection limit of 0.2 mg/L

The TF of AFFF was determined by combustion ion chromatography (CIC; Metrohm). AFFF was diluted 500 times with Milli-Q water. Diluted AFFF (100 μL) was decomposed at 1050 °C in the combustion module (Analytik Jena), and fluorine carried by argon gas was trapped by a 920 absorber module as $F^-$, which was quantified by IC (930 Compact IC Flex). The CIC measurement TF detection limit of 5 μg/L. Since no $F^-$ was detected in the AFFF, the TOF of AFFF samples equals their TF. Compared with other methods of TF estimation using targeted PFAS analysis (led to underreporting of TF[23]) and total oxidizable precursor assay (results subjected to digestion conditions[24]), CIC is the most suitable baseline for establishing a fluorine balance in this study. Details of sample preparation, equipment setup, and method detection limits of $F^-$, TOC, and TF analyses can be found in Text S6.

**Acknowledgments**

The authors thank the support of the U.S. National Science Foundation CAREER Award #2237080. The PFAS analysis is supported in part by the U.S. National Science Foundation Award #2120452. The authors thank Professor Jinyong Liu of the University of California at Riverside for providing the AFFF samples. The authors thank Dr. Adarsh N. Narayanan and Professor Mario Wriedt of Clarkson University for obtaining the BET surface area of BN.

## Data Availability

The data that support the findings of this study are available within the paper and its Supplementary Information. Source data for all graphs are provided with this paper. Mass spectrometry raw data are available from the corresponding author upon reasonable request.

## References


(1) Glüge, J.; Scheringer, M.; T. Cousins, I.; C. DeWitt, J.; Goldenman, G.; Herzke, D.; Lohmann, R.; A. Ng, C.; Trier, X.; Wang, Z. An Overview of the Uses of Per- and Polyfluoroalkyl Substances (PFAS). *Environ. Sci. Process. Impacts* **2020**, *22* (12), 2345–2373. https://doi.org/10.1039/D0EM00291G.

(2) Evich, M. G.; Davis, M. J. B.; McCord, J. P.; Acrey, B.; Awkerman, J. A.; Knappe, D. R. U.; Lindstrom, A. B.; Speth, T. F.; Tebes-Stevens, C.; Strynar, M. J.; Wang, Z.; Weber, E. J.; Henderson, W. M.; Washington, J. W. Per- and Polyfluoroalkyl Substances in the Environment. *Science* **2022**, *375* (6580), 16. https://doi.org/10.1126/science.abg9065.

(3) Awad, E.; Zhang, X.; Bhavsar, S. P.; Petro, S.; Crozier, P. W.; Reiner, E. J.; Fletcher, R.; Tittlemier, S. A.; Braekevelt, E. Long-Term Environmental Fate of Perfluorinated Compounds after Accidental Release at Toronto Airport. *Environ. Sci. Technol.* **2011**, *45* (19), 8081–8089. https://doi.org/10.1021/es2001985.

(4) Hu, X. C.; Andrews, D. Q.; Lindstrom, A. B.; Bruton, T. A.; Schaider, L. A.; Grandjean, P.; Lohmann, R.; Carignan, C. C.; Blum, A.; Balan, S. A.; Higgins, C. P.; Sunderland, E. M. Detection of Poly- and Perfluoroalkyl Substances (PFASs) in U.S. Drinking Water Linked to Industrial Sites, Military Fire Training Areas, and Wastewater Treatment Plants. *Environ. Sci. Technol. Lett.* **2016**, *3* (10), 344–350. https://doi.org/10.1021/acs.estlett.6b00260.

(5) Liu, M.; Munoz, G.; Vo Duy, S.; Sauvé, S.; Liu, J. Per- and Polyfluoroalkyl Substances in Contaminated Soil and Groundwater at Airports: A Canadian Case Study. *Environ. Sci. Technol.* **2022**, *56* (2), 885–895. https://doi.org/10.1021/acs.est.1c04798.

(6) Shields, E. P.; Krug, J. D.; Roberson, W. R.; Jackson, S. R.; Smeltz, M. G.; Allen, M. R.; Burnette, R. P.; Nash, J. T.; Virtaranta, L.; Preston, W.; Liberatore, H. K.; Wallace, M. A. G.; Ryan, J. V.; Kariher, P. H.; Lemieux, P. M.; Linak, W. P. Pilot-Scale Thermal Destruction of

Per- and Polyfluoroalkyl Substances in a Legacy Aqueous Film Forming Foam. *ACS EST Eng.* **2023**, *3* (9), 1308–1377. https://doi.org/10.1021/acsestengg.3c00098.

(7) United States, Department of Defense, Office of the Assistant Secretary of Defense. *Temporary Prohibition on Incineration of Materials Containing Per- and Polyfluoroalkyl Substances (PFAS)*. https://media.defense.gov/2022/Apr/28/2002986273/-1/-1/1/TEMPORARY-PROHIBITION-ON-INC%5B%E2%80%A6%5DNG-PRE-AND-POLYFLUOROALKYL-SUBSTANCES-PFAS-APRIL-26-2022.PDF (accessed 2023-12-12).

(8) Arana Juve, J.-M.; Wang, B.; Wong, M. S.; Ateia, M.; Wei, Z. Complete Defluorination of Per- and Polyfluoroalkyl Substances — Dream or Reality? *Curr. Opin. Chem. Eng.* **2023**, *41*, 100943. https://doi.org/10.1016/j.coche.2023.100943.

(9) Yang, S.; Fernando, S.; Holsen, T. M.; Yang, Y. Inhibition of Perchlorate Formation during the Electrochemical Oxidation of Perfluoroalkyl Acid in Groundwater. *Environ. Sci. Technol. Lett.* **2019**, *6* (12), 775–780. https://doi.org/10.1021/acs.estlett.9b00653.

(10) Bentel, M. J.; Yu, Y.; Xu, L.; Li, Z.; Wong, B. M.; Men, Y.; Liu, J. Defluorination of Per- and Polyfluoroalkyl Substances (PFASs) with Hydrated Electrons: Structural Dependence and Implications to PFAS Remediation and Management. *Environ. Sci. Technol.* **2019**, *53* (7), 3718–3728. https://doi.org/10.1021/acs.est.8b06648.

(11) Trang, B.; Li, Y.; Xue, X.-S.; Ateia, M.; Houk, K. N.; Dichtel, W. R. Low-Temperature Mineralization of Perfluorocarboxylic Acids. *Science* **2022**, *377* (6608), 839–845. https://doi.org/10.1126/science.abm8868.

(12) Young, R. B.; Pica, N. E.; Sharifan, H.; Chen, H.; Roth, H. K.; Blakney, G. T.; Borch, T.; Higgins, C. P.; Kornuc, J. J.; McKenna, A. M.; Blotevogel, J. PFAS Analysis with Ultrahigh Resolution 21T FT-ICR MS: Suspect and Nontargeted Screening with Unrivaled Mass Resolving Power and Accuracy. *Environ. Sci. Technol.* **2022**, *56* (4), 2455–2465. https://doi.org/10.1021/acs.est.1c08143.

(13) Bruton, T. A.; Sedlak, D. L. Treatment of Aqueous Film-Forming Foam by Heat-Activated Persulfate Under Conditions Representative of In Situ Chemical Oxidation. *Environ. Sci. Technol.* **2017**, *51* (23), 13878–13885. https://doi.org/10.1021/acs.est.7b03969.

(14) E. Schaefer, C.; Tran, D.; Fang, Y.; Jeong Choi, Y.; P. Higgins, C.; J. Strathmann, T. Electrochemical Treatment of Poly- and Perfluoroalkyl Substances in Brines. *Environ. Sci. Water Res. Technol.* **2020**, *6* (10), 2704–2712. https://doi.org/10.1039/D0EW00377H.

(15) Schaefer, C. E.; Choyke, S.; Ferguson, P. L.; Andaya, C.; Burant, A.; Maizel, A.; Strathmann, T. J.; Higgins, C. P. Electrochemical Transformations of Perfluoroalkyl Acid (PFAA) Precursors and PFAAs in Groundwater Impacted with Aqueous Film Forming Foams. *Environ. Sci. Technol.* **2018**, *52* (18), 10689–10697.

(16) Singh, R. K.; Multari, N.; Nau-Hix, C.; Anderson, R. H.; Richardson, S. D.; Holsen, T. M.; Mededovic Thagard, S. Rapid Removal of Poly- and Perfluorinated Compounds from Investigation-Derived Waste (IDW) in a Pilot-Scale Plasma Reactor. *Environ. Sci. Technol.* **2019**, *53* (19), 11375–11382. https://doi.org/10.1021/acs.est.9b02964.

(17) Tenorio, R.; Liu, J.; Xiao, X.; Maizel, A.; Higgins, C. P.; Schaefer, C. E.; Strathmann, T. J. Destruction of Per- and Polyfluoroalkyl Substances (PFASs) in Aqueous Film-Forming Foam (AFFF) with UV-Sulfite Photoreductive Treatment. *Environ. Sci. Technol.* **2020**, *54* (11), 6957–6967. https://doi.org/10.1021/acs.est.0c00961.

(18) Hao, S.; Choi, Y.-J.; Wu, B.; Higgins, C. P.; Deeb, R.; Strathmann, T. J. Hydrothermal Alkaline Treatment for Destruction of Per- and Polyfluoroalkyl Substances in Aqueous Film-Forming Foam. *Environ. Sci. Technol.* **2021**, *55* (5), 3283–3295. https://doi.org/10.1021/acs.est.0c06906.

(19) Zhang, K.; Huang, J.; Yu, G.; Zhang, Q.; Deng, S.; Wang, B. Destruction of Perfluorooctane Sulfonate (PFOS) and Perfluorooctanoic Acid (PFOA) by Ball Milling. *Environ. Sci. Technol.* **2013**, *47* (12), 6471–6477. https://doi.org/10.1021/es400346n.

(20) Turner, L. P.; Kueper, B. H.; Jaansalu, K. M.; Patch, D. J.; Battye, N.; El-Sharnouby, O.; Mumford, K. G.; Weber, K. P. Mechanochemical Remediation of Perfluorooctanesulfonic Acid (PFOS) and Perfluorooctanoic Acid (PFOA) Amended Sand and Aqueous Film-Forming Foam (AFFF) Impacted Soil by Planetary Ball Milling. *Sci. Total Environ.* **2021**, *765*, 142722. https://doi.org/10.1016/j.scitotenv.2020.142722.

(21) Gobindlal, K.; Zujovic, Z.; Jaine, J.; Weber, C. C.; Sperry, J. Solvent-Free, Ambient Temperature and Pressure Destruction of Perfluorosulfonic Acids under Mechanochemical Conditions: Degradation Intermediates and Fluorine Fate. *Environ. Sci. Technol.* **2023**, *57* (1), 277–285. https://doi.org/10.1021/acs.est.2c06673.

(22) Yang, N.; Yang, S.; Ma, Q.; Beltran, C.; Guan, Y.; Morsey, M.; Brown, E.; Fernando, S.; Holsen, T. M.; Zhang, W.; Yang, Y. Solvent-Free Nonthermal Destruction of PFAS Chemicals and PFAS in Sediment by Piezoelectric Ball Milling. *Environ. Sci. Technol. Lett.* **2023**, *10* (2), 198–203. https://doi.org/10.1021/acs.estlett.2c00902.

(23) Dubocq, F.; Wang, T.; Yeung, L. W. Y.; Sjöberg, V.; Kärrman, A. Characterization of the Chemical Contents of Fluorinated and Fluorine-Free Firefighting Foams Using a Novel Workflow Combining Nontarget Screening and Total Fluorine Analysis. *Environ. Sci. Technol.* **2020**, *54* (1), 245–254. https://doi.org/10.1021/acs.est.9b05440.

(24) Ateia, M.; Chiang, D.; Cashman, M.; Acheson, C. Total Oxidizable Precursor (TOP) Assay─Best Practices, Capabilities and Limitations for PFAS Site Investigation and Remediation. *Environ. Sci. Technol. Lett.* **2023**, *10* (4), 292–301. https://doi.org/10.1021/acs.estlett.3c00061.

(25) US EPA, O. *CWA Analytical Methods for Per- and Polyfluorinated Alkyl Substances (PFAS)*. https://www.epa.gov/cwa-methods/cwa-analytical-methods-and-polyfluorinated-alkyl-substances-pfas (accessed 2023-10-27).

(26) Gobindlal, K.; Zujovic, Z.; Yadav, P.; Sperry, J.; Weber, C. C. The Mechanism of Surface-Radical Generation and Amorphization of Crystalline Quartz Sand upon Mechanochemical Grinding. *J. Phys. Chem. C* **2021**, *125* (38), 20877–20886. https://doi.org/10.1021/acs.jpcc.1c06069.

(27) Narayanasamy, J.; Kubicki, J. D. Mechanism of Hydroxyl Radical Generation from a Silica Surface: Molecular Orbital Calculations. *J. Phys. Chem. B* **2005**, *109* (46), 21796–21807. https://doi.org/10.1021/jp0543025.

(28) Turner, L. P.; Kueper, B. H.; Patch, D. J.; Weber, K. P. Elucidating the Relationship between PFOA and PFOS Destruction, Particle Size and Electron Generation in Amended Media Commonly Found in Soils. *Sci. Total Environ.* **2023**, *888*, 164188. https://doi.org/10.1016/j.scitotenv.2023.164188.

(29) Gao, J.; Liu, Z.; Chen, Z.; Rao, D.; Che, S.; Gu, C.; Men, Y.; Huang, J.; Liu, J. Photochemical Degradation Pathways and Near-Complete Defluorination of Chlorinated Polyfluoroalkyl Substances. *Nat. Water* **2023**, *1*, 381–390. https://doi.org/10.1038/s44221-023-00046-z.

(30) Luo, Y.; Khoshyan, A.; Al Amin, M.; Nolan, A.; Robinson, F.; Fenstermacher, J.; Niu, J.; Megharaj, M.; Naidu, R.; Fang, C. Ultrasound-Enhanced Magnéli Phase Ti4O7 Anodic

Oxidation of per- and Polyfluoroalkyl Substances (PFAS) towards Remediation of Aqueous Film Forming Foams (AFFF). *Sci. Total Environ.* **2023**, *862*, 160836. https://doi.org/10.1016/j.scitotenv.2022.160836.

(31) Prevedouros, K.; Cousins, I. T.; Buck, R. C.; Korzeniowski, S. H. Sources, Fate and Transport of Perfluorocarboxylates. *Environ. Sci. Technol.* **2006**, *40* (1), 32–44. https://doi.org/10.1021/es0512475.

(32) Houtz, E. F.; Higgins, C. P.; Field, J. A.; Sedlak, D. L. Persistence of Perfluoroalkyl Acid Precursors in AFFF-Impacted Groundwater and Soil. *Environ. Sci. Technol.* **2013**, *47* (15), 8187–8195. https://doi.org/10.1021/es4018877.

(33) Nickerson, A.; Rodowa, A. E.; Adamson, D. T.; Field, J. A.; Kulkarni, P. R.; Kornuc, J. J.; Higgins, C. P. Spatial Trends of Anionic, Zwitterionic, and Cationic PFASs at an AFFF-Impacted Site. *Environ. Sci. Technol.* **2021**, *55* (1), 313–323. https://doi.org/10.1021/acs.est.0c04473.

(34) Mori, H.; Mio, H.; Kano, J.; Saito, F. Ball Mill Simulation in Wet Grinding Using a Tumbling Mill and Its Correlation to Grinding Rate. *Powder Technol.* **2004**, *143–144*, 230–239. https://doi.org/10.1016/j.powtec.2004.04.029.

(35) James, S. L.; Adams, C. J.; Bolm, C.; Braga, D.; Collier, P.; Friščić, T.; Grepioni, F.; Harris, K. D. M.; Hyett, G.; Jones, W.; Krebs, A.; Mack, J.; Maini, L.; Orpen, A. G.; Parkin, I. P.; Shearouse, W. C.; Steed, J. W.; Waddell, D. C. Mechanochemistry: Opportunities for New and Cleaner Synthesis. *Chem. Soc. Rev.* **2011**, *41* (1), 413–447. https://doi.org/10.1039/C1CS15171A.

(36) Xiao, F.; Sasi, P. C.; Yao, B.; Kubátová, A.; Golovko, S. A.; Golovko, M. Y.; Soli, D. Thermal Stability and Decomposition of Perfluoroalkyl Substances on Spent Granular Activated Carbon. *Environ. Sci. Technol. Lett.* **2020**, *7* (5), 343–350. https://doi.org/10.1021/acs.estlett.0c00114.

(37) Li, L. H.; Chen, Y. Superhydrophobic Properties of Nonaligned Boron Nitride Nanotube Films. *Langmuir* **2010**, *26* (7), 5135–5140. https://doi.org/10.1021/la903604w.

(38) Yadav, V.; Kulshrestha, V. Boron Nitride: A Promising Material for Proton Exchange Membranes for Energy Applications. *Nanoscale* **2019**, *11* (27), 12755–12773. https://doi.org/10.1039/C9NR03094H.

(39) Vohera, H. *How Hard is Stainless Steel - A Complete Guide*. ThePipingMart Blog. https://blog.thepipingmart.com/metals/how-hard-is-stainless-steel-a-complete-guide/ (accessed 2023-07-16).

(40) *The Mohs Hardness Scale And Chart For Select Gems*. International Gem Society. https://www.gemsociety.org/article/select-gems-ordered-mohs-hardness/ (accessed 2023-07-16).

(41) Chen, X.; Wu, P.; Rousseas, M.; Okawa, D.; Gartner, Z.; Zettl, A.; Bertozzi, C. R. Boron Nitride Nanotubes Are Noncytotoxic and Can Be Functionalized for Interaction with Proteins and Cells. *J. Am. Chem. Soc.* **2009**, *131* (3), 890–891. https://doi.org/10.1021/ja807334b.